

# PRAFOR - updating hydrological balance

Aaron M

26 November 2020

## Contents

<b>1</b>	<b>Updating the FR 3PG model with improved hydrological sub-models</b>	<b>1</b>
1.1	Hydrological balance equation . . . . .	1
1.2	Soil water content and available soil water . . . . .	2
1.3	Soil evaporation . . . . .	3
<b>2</b>	<b>Abridged outline of hydrology sub-models in FR 3PG</b>	<b>4</b>
<b>3</b>	<b>Calibration</b>	<b>6</b>
3.1	Data . . . . .	6
3.2	Likelihood function . . . . .	7
3.3	Priors . . . . .	7
3.4	MCMC algorithm . . . . .	7
<b>4</b>	<b>Spatial analysis</b>	<b>7</b>
	<b>References</b>	<b>9</b>

## 1 Updating the FR 3PG model with improved hydrological sub-models

A key limitation in the original 3PG model when considering drought, is its relatively simplistic approach to soil hydrology. Principally, this has implications for accurate simulation of ecophysiological processes in tree plantations, e.g. under-estimation of evapotranspiration. Therefore, productivity outputs during drought periods are potentially erroneous.

To overcome these limitations, a new set of hydrological balance equations were proposed and validated by Almedia and Sands (2016). These build on the original 3PG hydrology by including finer-scale processes which drive soil water content and evaporation.

To build on the FR 3PG model, which includes additional soil respiration and decomposition functions described by Xenakis et al., we have incorporated the proposed hydrological sub-models as described below.

### 1.1 Hydrological balance equation

The hydrological balance in the 3PG model specifies changes to the soil water content SWC ( $\Theta$ ) within a discrete time period ( $\delta t$ ).

$$\Theta(t + \delta t) = \Theta(t) + R - I_R - E_C - E_S - q_D - q_R \quad (1)$$

Where:

$R$  = Rainfall (mm)

$I_R$  = The rainfall intercepted by the canopy (mm)

$E_C$  = Canopy transpiration (mm)

$E_S$  = Evaporation from the soil (mm)

$q_R$  = Surface run-off (mm)

In our version of the 3PG, rainfall is calculated from meteorological observations, and rainfall interception, canopy transpiration and surface run-off are calculated as originally described by Landsberg and Waring (1997). Whilst Almedia and Sands provide updated equations for surface run-off when soil is saturated, as we are focusing on times where water content is low, we have not implemented these updates yet.

## 1.2 Soil water content and available soil water

Considering the hydrological balance equation for  $\Theta(t + \delta t)$  (eq. 1). if the rooting zone  $Z_R$  (m) is the depth of soil occupied by the trees roots (and hence water in this zone is available for uptake), the volumetric soil water content SWC  $\theta$  ( $m^3m^{-3}$ ) can be considered  $\frac{\Theta}{z}$ .

The relative plant available soil water ASW in the rooting zone ( $\theta_r$ ) is then the ratio of the current plant ASW to the maximum ASW, derived from the wilting point ( $\theta_{wp}$ ) and field capacity ( $\theta_{fc}$ ) of the soil profile:

$$\theta_r = \frac{\theta - \theta_{wp}}{\theta_{fc} - \theta_{wp}} \quad (2)$$

The value of  $\theta_r$  is bounded between 0-1 and drives tree growth and decomposition in the soil by modifying the soil water growth modifier ( $f_\theta$ ).

$$f_\theta = \frac{1 - (1 - \theta_r)^{n_\theta}}{1 + (1 - 2c_\theta^{n_\theta})[(1 - \theta_r)/c_\theta]^{n_\theta}} \quad (3)$$

Where  $c_\theta$  and  $n_\theta$  are texture dependant soil parameters.

Almedia and Sands (2016) describes two zones in the soil profile, the root zone ( $z_R$ ) and non-root zone ( $z_{nR}$ ). The root zone, can be derived from the allocation of biomass to the roots,  $z_R = \min[\sigma_{zR} W_r 0.1, Z_{nR}]$ , where  $W_r$  is the biomass allocated to roots,  $\sigma_{zR}$  is a modifier for the volume of soil explored per kg of root biomass and it is assumed that it's maximum volume is that of the non-root zone (this could be replaced with a maximum rooting depth).

Water moves from one zone to the next along the water pressure gradient, dependent on the SWC of the rooting and non-rooting zones at the beginning of the time-step ( $\Theta_{rz0}$  and  $\Theta_{nr0}$  respectively) and the volume of the root-zone ( $V_{rz}$ ) and non-root ( $V_{nr}$ ).

$$\Theta_{rz}(t) = \frac{\Theta_{rz0}V_{nr} - \Theta_{nr0}V_{rz}}{V_{rz} + V_{nr}}e^{-t/t_{s0}} + \frac{V_r z}{V_r z + V_{nr}}(\Theta_{rz0} + \Theta_{nr0}) \quad (4)$$

Where  $t_{S0}$  is the time constant for water movement based on the conductivity of the soil  $K_S$  and assuming both zones have a shared area  $A(m^2)$ :

$$t_{S0} = \frac{V_{rz}V_{nr}}{K_S A(V_{rz} + V_{nr})} \quad (5)$$

### 1.3 Soil evaporation

Soil evaporation rate ( $E_S$ ) is split into two phases, following a model by Ritchie (1972). In phase 1, an upper layer of soil is assumed to act as a barrier to further evaporation below the surface, forming a protective layer as it dries. Therefore, evaporation occurs at a maximum potential rate ( $e_0$ ) directly after a wetting event, until a threshold value ( $E_{S1}$ ) is reached and the upper layer has dried out. Subsequently in phase 2, evaporation rate slows hyperbolically at a rate based on soil texture ( $E_{S2}$ ) (Figure 2).

If the duration of phase 1 is  $t_{S1} = E_{S1}/e_0$  the value of  $E_S(t)$  can be considered:

$$E_S(t) = \begin{cases} e_0 t & t \leq t_{S1} \\ E_{S1} + E_{S2}(\sqrt{(1 + 2(e_0/E_{S2})(t - t_{S1}) - 1}) & t > t_{S1} \end{cases} \quad (6)$$

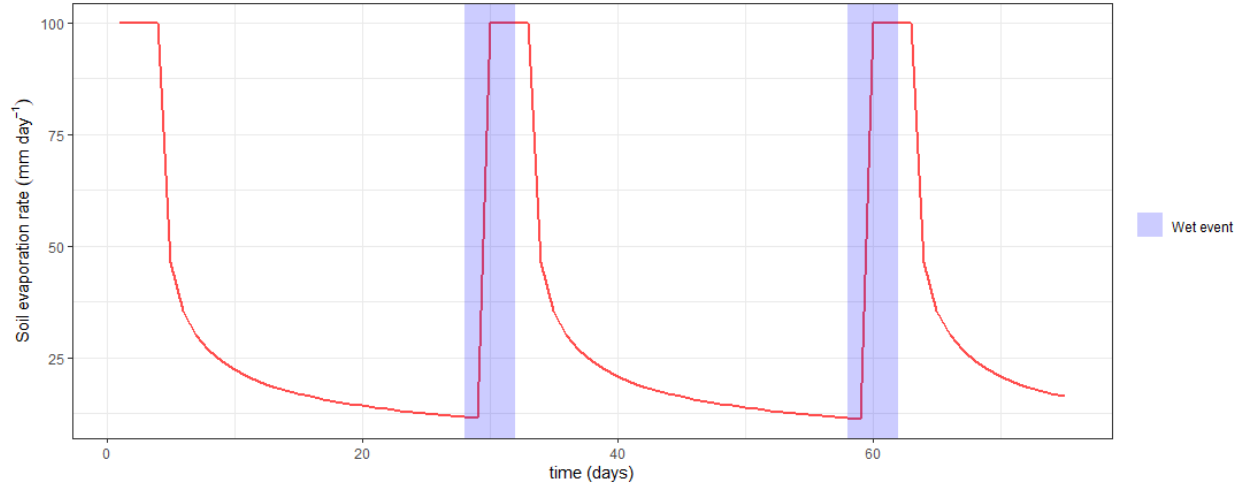


Figure 2. Soil evaporation rate  $E_S$  (mm) is shown over time. The blue shaded areas represent wetting events, after such an event,  $E_S$  occurs at the maximum potential rate  $e_0$  (mm day<sup>-1</sup>) until a threshold cumulative value  $E_{S1}$  (mm) is reached.  $E_S$  then declines hyperbolically at a rate based on soil texture  $E_{S2}$  until another wetting event occurs, which reduces the cumulative  $E_S$  by the volume of water input in mm. For clarity, this figure assumes the cumulative value  $E_S$  has reached zero before the next wetting event

The maximum potential evaporation rate ( $e_0$ ) is calculated using a Penman-Monteith equation driven by solar radiation reaching the soil and the vapor pressure deficit (VPD) above the soil. Aerodynamic boundary layer conductance  $g_{as}$  is lower than at the canopy at approximately  $0.01g_{ac}$ , and soil surface conductance  $g_{Ac}$  in place of canopy conductance is considered infinite (Almeida and Sands 2016). Solar radiation reaching the soil ( $\varphi_{sr}$ ) is a factor of the amount of radiation absorbed by the canopy  $\varphi_{na}$ . Where, following Beers law, which estimates the amount of radiation absorbed by a material,  $\varphi_{na} = a + b\varphi_i$ , where  $a$  and  $b$  have values for sitka plantations of -90 and 0.8 respectively (F. Minunno et al. 2010).  $\varphi_i$  is driven by the daily

insolation  $Q(MJm^{-2}day^{-1})$  over the day length ( $h$ ), the leaf area index ( $L$ ) and the extinction coefficient for absorption of photosynthetic active radiation (PAR) by the canopy ( $k$ ) (Figure 3), thus:

$$\varphi_i = 10^6 \frac{Q}{h} (1 - e^{(-kL)}) \quad (7)$$

and

$$\varphi_{sr} = 10^6 \frac{Q}{h} - \varphi_{na}. \quad (8)$$

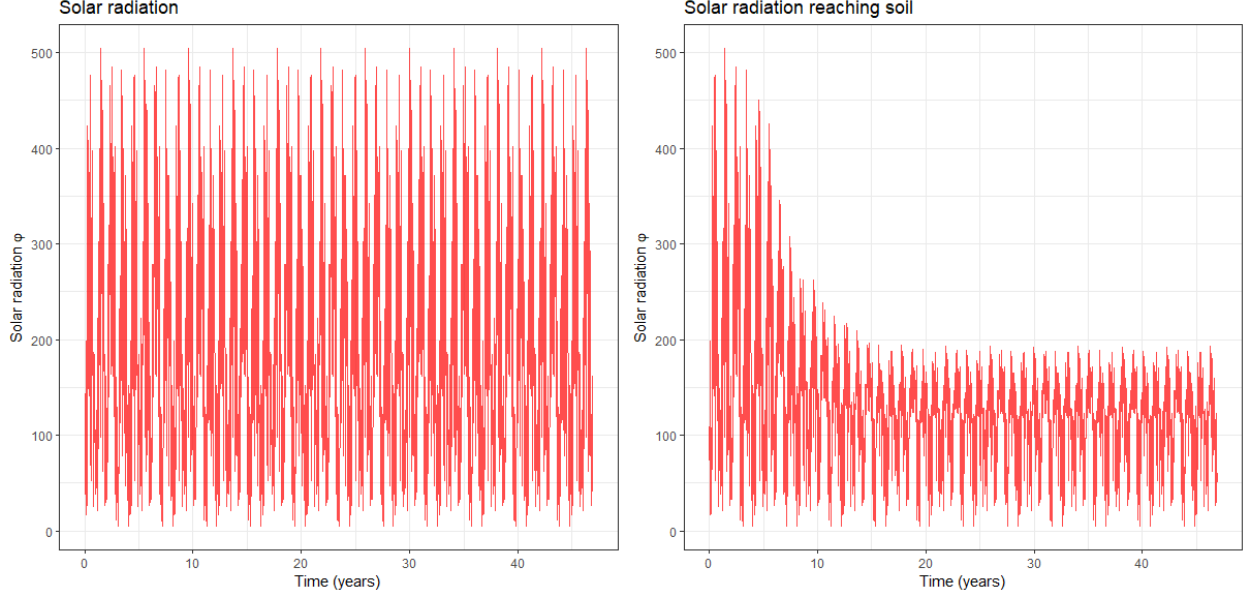


Figure 3. Total solar radiation occurring in weekly time-steps over Harwood forest plantation, and the solar radiation reaching the soil reduced by canopy absorption. As the trees grow over time, canopy size increases reducing the amount of solar radiation that is able to reach the soil.

To calculate the volume of water evaporated during a time-step, we take the cumulative value at the beginning of the time-step and consider this  $E_{S0}$ , by re-arranging the equation for  $E_S(t)$  for  $t$  we can get a corresponding value of  $t_0$ :

$$t_0 = (-2E_{S0}E_{S1}) + (E_{S0}^2) + (2E_{S0}) + (E_{S1}^2) - (2E_{S1}) + 1 + (2e0E_{S2}t_{s1} - (E_{S2}^2)) \quad (9)$$

Thus, the soil evaporation during the time-step can be derived as:

$$E_S(t_0 + \delta t) - E_{S0} \quad (10)$$

## 2 Abridged outline of hydrology sub-models in FR 3PG

A schematic of the updated hydrological sub-models is shown in figure 4. The incorporation of the submodels specifically into the current FR implementation of the 3PG is described below. For clarity, only the updated

hydrological sub-models are explained in detail.

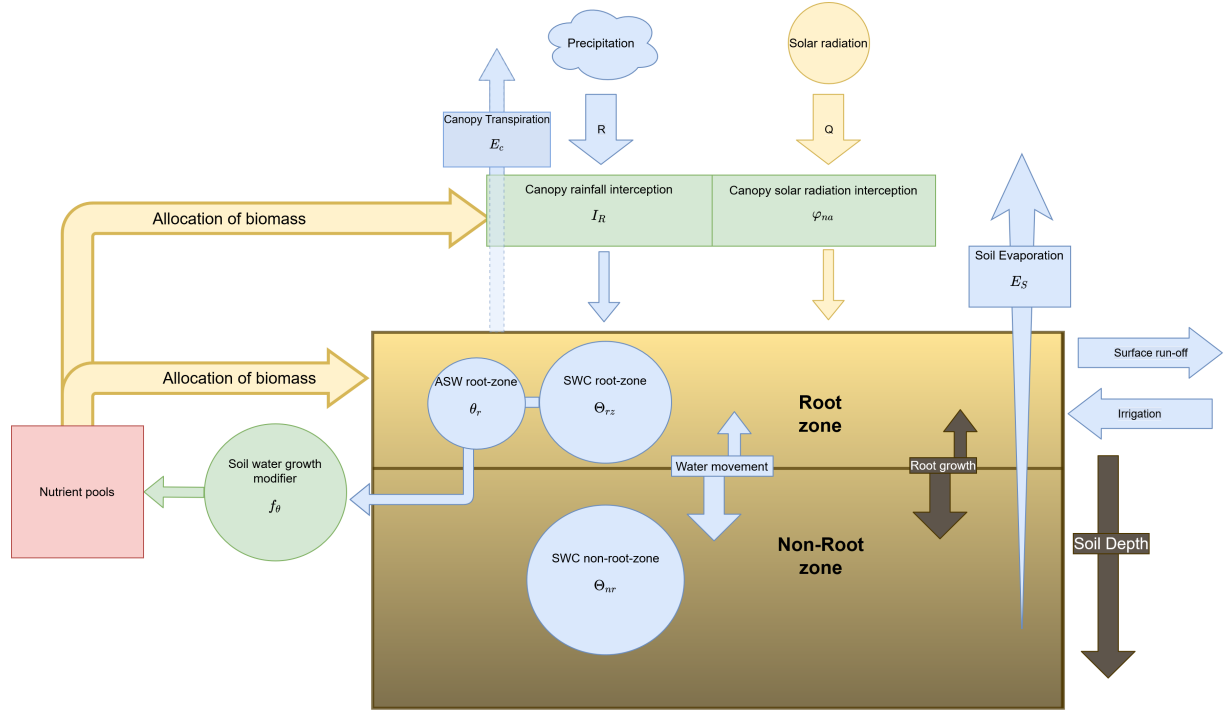


Figure 4. Schematic diagram of the hydrological balance submodel based on Almedia and Sands (2016).

The FR 3PG model runs in discrete time-steps ( $\delta t$ ), during each time-step, states of the trees/stand (e.g. biomass) are updated based on the states at the end of the previous time-step, parameter values and calculated modifiers.

⇒ **Start of time-step in FR 3PG model**

⇒ Estimate solar radiation and interception

⇒ Calculate modifiers

⇒ Estimate productivity

⇒ **Update soil water content (SWC) for rooting zone**

- Refer to section 1.2 for full details.
- Estimate current depth of rooting zone  $z_R$  (m) from root biomass ( $W_r$ ) at the end of previous time-step and parameter  $\sigma_{zR}$  which dictates the volume of soil explored by 1kg of root biomass

$$z_R = \min[\sigma_{zR} W_r 0.1, Z_{nR}]$$

(0.1 is a conversion from tons per hectare to kg per square meter)

- Estimate volumetric SWC of the root zone at wilting point  $\theta_{wp}$  (mm) and field capacity  $\theta_{fc}$  (mm) based on root-zone size and soil attributes

$$\theta_{wp} = w_p \sigma_{zR} W_r 100$$

$$\theta_{fc} = f_c \sigma_{zR} W_r 100$$

(multiplying by 100 is to convert values to mm)

- Calculate maximum available soil water ( $\Theta_{max}$ ) based on field capacity and wilting point  $\Theta_{max} = \theta_{fc} - \theta_{wp}$
- Calculate SWC of the rooting zone  $\Theta_{rz}$  for the end of the time-step, but before the addition of rainfall and irrigation. As described by Almedia and Sands (2016) SWC at the end of the time-step can be derived using the SWC of the rooting zone and non-rooting zone at the start of the time-step ( $\Theta_{rz0}, \Theta_{nr0}$ ), the size of the root-zone ( $V_{rz}$ ) and non-root ( $V_{nr}$ ), the length of the time-step in days ( $\delta t$ ) and soil water conductivity ( $K_s$ ) (see eq. 4).
- Calculate available soil water  $\theta_r$

$$\theta_r = \frac{\theta - \theta_{wp}}{\theta_{fc} - \theta_{wp}}$$

⇒ **Calculate the volume of water evaporation from soil during the time-step**

- Refer to section 1.3 for full details.
- Calculate the potential rate of evaporation ( $e_0$ ) using the Penman-Monteith equation, where aerodynamic boundary layer conductance is lower than at the canopy, and surface conductance is considered infinite. Radiation reaching the ground during the time-step is reduced by canopy cover based on leaf area index (LAI) and canopy absorption.
- Using soil property parameters, the length of time-step ( $\delta t$ ) and the potential evaporation rate ( $e_0$ ), calculate the amount of moisture lost during the time-step in two stages:
  1. Surface evaporation occurs at the potential evaporation rate ( $e_0$ ) until a cumulative threshold value ( $E_{S1}$ ) is reached, suggesting that the surface layer has dried out
  2. As water deeper in the soil profile becomes less accessible to solar radiation, evaporation rate declines from the potential value hyperbolically, dependent on soil texture parameters. Cumulative evaporation is stored, minus throughfall and irrigation.
- Calculate excess soil water

⇒ **Update SWC for non-rooting zone**

- Size of non-rooting zone is a set maximum value minus the size of the rooting zone
- The SWC of the non-rooting zone is derived by re-arranging the equation for the rooting zone SWC calculation (eq. 4)

⇒ **Add weekly rainfall and irrigation, minus evaporation, transpiration and excess water to the root zone SWC**

- Allocate biomass based on ASW etc.
- Estimate mortality
- Update soil nutrients and decomposition
- Predict useful state variables e.g. LAI
- End of time step, repeat.

## 3 Calibration

### 3.1 Data

Data for calibration and validation of the modified 3-PGN model, came from 51 experimental plots of Scots pine, receiving different silvicultural treatments, and were part of the UK Forestry Commission permanent sample plot (PSP) data base. Validation of the model simulations has been recently applied to new data from the Harwood forest site, which has monthly recording of fluxes between 2015 and 2018.

Model runs on monthly, weekly or daily time-steps where data is available.

### 3.2 Likelihood function

Calibration of the model followed similar methods to previous publications including Minunno et al (2010) and Xenakis et al. (2020) (unpublished) using likelihood based MCMC algorithms. Here we defined the likelihood function based around a normal distribution, where for the data  $y$  with mean  $\mu$  and S.D.  $\sigma$ , a vector of parameters  $\theta$  and simulated value  $x$ ,

$$p(y(\mu, \sigma)|x, \theta) = \frac{1}{\sqrt{(2\pi)}\sigma} e^{-\frac{(x-\mu)^2}{2\sigma^2}} \quad (11)$$

Thus for observed data  $y_{1:t}$  the full likelihood value can be considered:

$$\mathcal{L}(\theta|y_{1:t}) = \prod_{n=1}^t p(y_n|x_n, \theta) \quad (12)$$

### 3.3 Priors

Priors for calibration were uniform... (need to add table of priors)

### 3.4 MCMC algorithm

We used a Differential-Evolution MCMC (Braak and Vrugt 2008) in the BayesianTools R package (Hartig, Minunno, and Paul 2018), which utilises a genetic algorithm for chains to learn from each-other as they progress, in addition to a snooker updater. We run the MCMC algorithm for  $x$  number of iterations with  $n$  chains and a burn-in period of 10%.

Calibration yet to be fully run, completing setup on JASMIN cluster.

## 4 Spatial analysis

As part of the PRAFOR project we aim to apply the calibrated FR 3PG model to spatial climatic and environmental data.

As proof of principle, we have developed a framework to apply the model to 1km or 5km grid-square longitudinal climatic data from CEDA (figure 5). This outputs the “potential” productivity of each grid-square which can then subsequently be plotted as a map (figure 6).

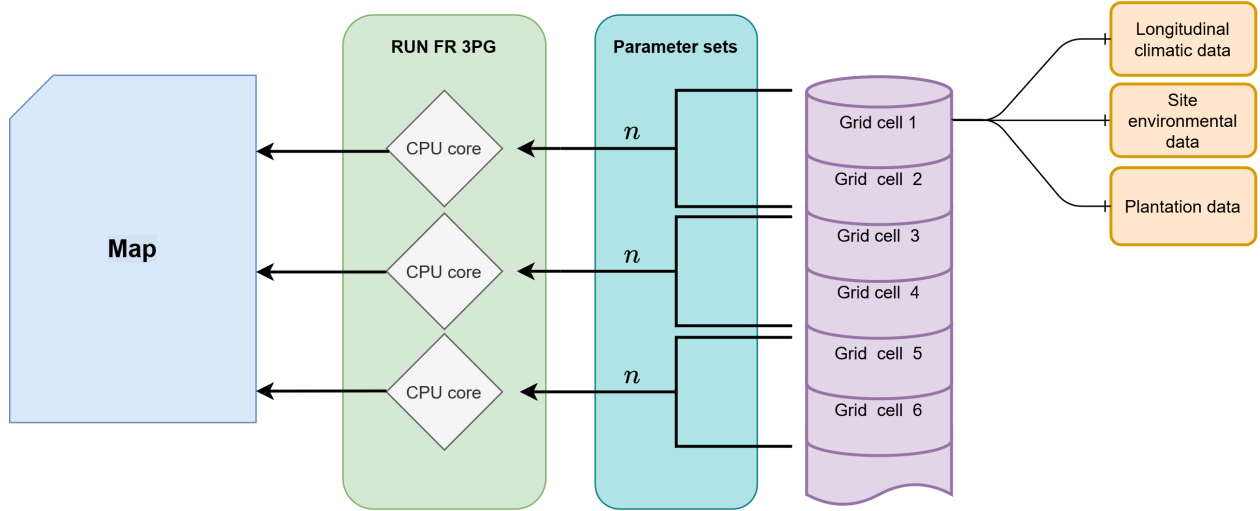


Figure 5 Schematic of spatial modelling framework, here showing how the data from six grid cells is processed in parallel accross multiple cpu cores. For each grid cell, the FR 3PG model is also run for  $n$  parameter sets sampled from the posterior of the MCMC calibration, enabling the calculation of an average and 95% CI range for the output. The output (e.g. biomass) is then plotted as a map using the georeferenced locations associated with each cell.

For each grid-square we run the FR3PG model with multiple parameter sets sampled from the posterior distribution. of the MCMC calibration. From this we take an average value and 95% credible intervals as a measure of uncertainty

The framework is flexible in that it allows us to attach any additional grid-referenced data to a corresponding grid square, e.g. soil type, current land use etc. Further, replacing grid squares with polygons for individual forests would be relatively trivial. Computationally, running the model for this number of locations and parameter sets is intensive (e.g. for 500 parameter sets and 100,000 grid squares would be 50 million runs of the model), however the framework is developed for parallel computation, and is highly scaleable, with each grid square able to be run on a seperate core. Utilising the batch computing facilities of JASMIN, it should be possible to undertake runs for the entire UK in relatively short periods.



Spatial analysis of FR3PG model - Scotland

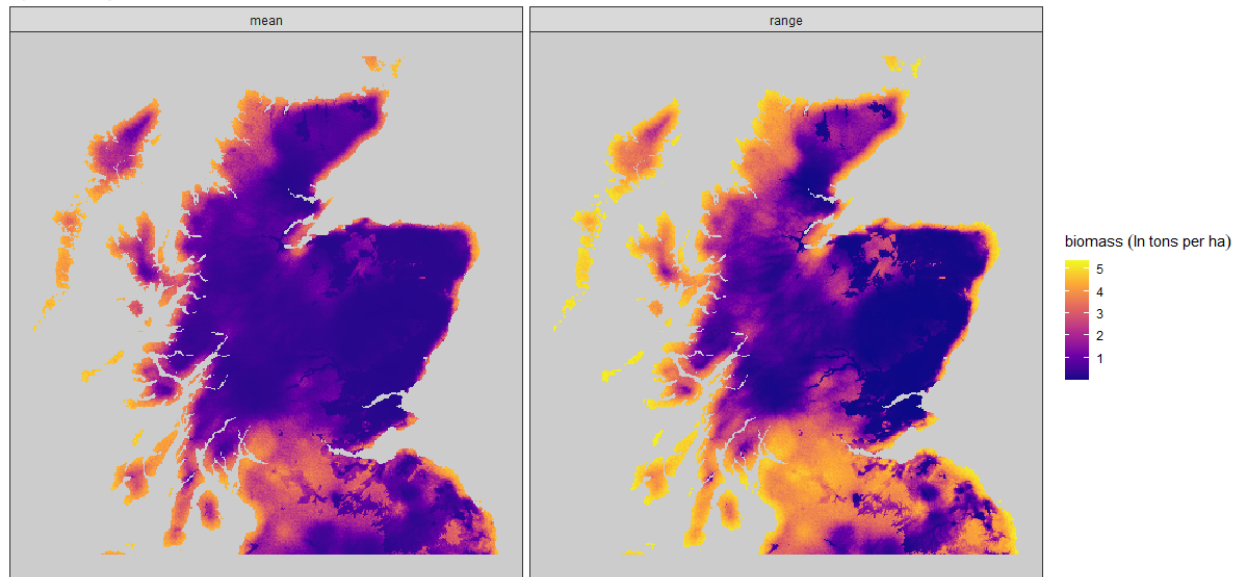


Figure 6 Example spatial analysis conducted using FR 3PG model with updated hydrological sub-models for 1km grid cells of climatic data taken from CEDA for part of Scotland. Note: Mean values are likely inaccurate and ranges are quite high as model has yet to be properly calibrated with hydrological sub-models

## References

- Almeida, Auro C, and Peter J Sands. 2016. "Improving the Ability of 3-Pg to Model the Water Balance of Forest Plantations in Contrasting Environments." *Ecohydrology* 9 (4). Wiley Online Library: 610–30.
- Braak, Cajo JF ter, and Jasper A Vrugt. 2008. "Differential Evolution Markov Chain with Snooker Updater and Fewer Chains." *Statistics and Computing* 18 (4). Springer: 435–46.
- Hartig, F, F Minunno, and S Paul. 2018. "BayesianTools: General-Purpose Mcmc and Smc Samplers and Tools for Bayesian Statistics, R Package Version 0.1. 3."
- Minunno, Francesco, Georgios Xenakis, Michael P Perks, and Maurizio Mencuccini. 2010. "Calibration and Validation of a Simplified Process-Based Model for the Prediction of the Carbon Balance of Scottish Sitka Spruce (*Picea Sitchensis*) Plantations." *Canadian Journal of Forest Research* 40 (12). NRC Research Press: 2411–26.